

# Alterations in Gold Nanoparticle Levels Are Size Dependent, with the Smaller Ones Inducing the Most Toxic Effects and Related to the Time of Exposure of the Gold Nanoparticles

MAK Abdelhalim

## ABSTRACT

**Background:** Gold nanoparticle (GNP) levels in the blood of rats *in vivo* have not been previously documented. This study aimed to evaluate the influence of size and exposure duration of GNPs on the gold levels in the blood of rats *in vivo*.

**Methods:** Thirty rats were divided into five groups, NG = control group, G1A: infusion of 10 nm GNPs for three days, G1B: 10 nm GNPs for seven days, G2A: 50 nm GNPs for three days and G2B: 50 nm GNPs for seven days. Fifty microlitres of GNPs dissolved in aqueous solution were administered intraperitoneally every day for three and seven days. Gold concentrations in different samples were measured using inductively coupled plasma-optical emission spectrometer (ICP-OES).

**Results:** The percentage normalized value of 50nm GNPs increased in the blood of rats in both three and seven days when compared with 10 nm GNPs.

**Conclusions:** It became evident from the results of this study that the alterations in GNP levels were size dependent, with the smaller ones inducing the most toxic effects and related to the time of exposure of GNPs. The results might indicate that the smaller GNPs are mostly taken up and accumulate in the different rat organs, suggesting their toxic effects, while the 50 nm GNPs are retained in the blood of rats for a long time. These conclusions are further supported by the histological investigation.

**Keywords:** Blood of rats, cancer, exposure duration, gold nanoparticles, *in vivo*

# Las Alteraciones en los Niveles de Nanopartículas de Oro Son Dependientes del Tamaño, Induciendo las Más Pequeñas los Efectos Más Tóxicos, y Guardan Relación con el Tiempo de Exposición de las Nanopartículas de Oro

MAK Abdelhalim

## RESUMEN

**Antecedentes:** Los niveles de nanopartículas de oro (AuNP) niveles en la sangre de ratas *in vivo* no han sido documentados con anterioridad. Este estudio persigue evaluar la influencia del tamaño y la duración de la exposición de las AuNP sobre los niveles de oro en la sangre de ratas *in vivo*.

**Métodos:** Treinta ratas fueron divididas en cinco grupos: NG = grupo de control, G1A = infusión de 10 nm de AuNP durante tres días, G1B = 10 nm de AuNP durante siete días, G2A = 50 nm de AuNP durante tres días, y G2B = 50 nm de AuNP durante siete días. Cincuenta microlitros de AuNP disueltos en solución acuosa fueron administrados por vía intraperitoneal todos los días durante tres y siete días. Las concentraciones de oro en diferentes muestras se midieron con el espectrómetro de emisión óptica de plasma acoplado inductivamente (ICP-OES).

**Resultados:** El valor de porcentaje normalizado de 50 nm de AuNP aumenta en la sangre de las ratas en tres y siete días en comparación con el AuNP de nm 10.

**Conclusiones:** A partir de los resultados de este estudio, se hizo evidente que las alteraciones en los niveles de AuNP son en primer lugar dependientes del tamaño, induciendo las más pequeñas los efectos más tóxicos, y en segundo lugar guardan relación con el tiempo de exposición de las AuNP. Los resulta-

*dos podrían indicar que las AuNP más pequeñas son en su mayoría absorbidas, acumulándose en los diferentes órganos de las ratas, lo que sugiere sus efectos tóxicos, mientras que por otra parte las AuNP de 50 nm son retenidas en la sangre de las ratas durante mucho tiempo. Estas conclusiones son además avaladas por la investigación histológica.*

**Palabras claves:** Sangre de ratas, duración de la exposición, cáncer, nanopartículas de oro, *in vivo*

West Indian Med J 2016; 65 (1): 88

## INTRODUCTION

The use of gold nanoparticles (GNPs) for detecting and treating cancer is a new and exciting field of research. The current methods of cancer diagnosis and treatment are costly and can be harmful to the body. Gold nanoparticles, however, offer an inexpensive route to targeting cancerous cells (1).

The particle size-dependent distribution of GNPs by organ has been studied *in vivo* (2–5). Orally administered GNPs appeared in various organs in mice and the absorbance and distribution were inversely correlated with the particle size (2). The small size of GNPs results in physical and chemical properties that are very different from those of the same material in the bulk form. These properties include a large surface to volume ratio, enhanced or hindered particle aggregation depending on the type of surface modification, enhanced photoemission, high electrical and heat conductivity and improved surface catalytic activity (6–9).

Toxicity has been thought to originate from nanomaterial size and surface area, composition and shape. The nanoparticle size plays a role in how the body responds to, distributes and eliminates materials (2, 5). The particle size can also affect the mode of endocytosis, cellular uptake and the efficiency of particle processing in the endocytic pathway (10, 11). The GNPs show several features that make them well suited for biomedical applications, including straightforward synthesis, stability and the potential for surface modification with active biological molecules such as peptides or proteins (12). Semmler-Behnke *et al* have observed that a considerable percentage of 18 nm GNPs are removed from the blood and are trapped predominantly in the liver and spleen (13).

The GNPs can be used in various biomedical applications; however, very little is known about their particle size and exposure duration dependence *in vivo*. To explore the potential role of GNPs in therapeutic and diagnostic applications, we evaluated the levels of different GNP sizes for periods of three and seven days following intraperitoneal administration in rats.

## SUBJECTS AND METHODS

Gold nanoparticles of different sizes (10 and 50 nm; MKN-Au-010 and MKN-Au-050, respectively; MK Impex Corp, Mississauga, Canada) were purchased and used in this study. The mean size and morphology of GNPs were evaluated using transmission electron microscopy (TEM).

## Animals

Healthy male Wistar-Kyoto rats were obtained from the Laboratory Animal Center (College of Pharmacy, King Saud University). The rats were 8–12 weeks old (approximately 250 g body weight) and housed in pairs in humidity and temperature-controlled ventilated cages on a 12-hour day/night cycle. Thirty rats were divided as follows: control group (NG: n = 10), G1A: infusion of 10 nm GNPs for three days; n = 5; G1B: 10 nm GNPs for seven days; n = 5; G2A: 50 nm GNPs for three days; n = 5 and G2B: 50 nm GNPs for seven days; n = 5. Fifty microlitres of GNPs dissolved in aqueous solution were only administered intraperitoneally to the rat-treated groups (G1A, G1B, G2A and G2B) for three and seven days; while the control rat group was not administered GNPs and/or aqueous solution. All experiments were conducted in accordance with the guidelines approved by King Saud University Local Animal Care and Use Committee.

## Inductively coupled plasma optical emission spectrometer

Inductively coupled plasma optical emission spectrometry (ICP-OES) was designed to determine the composition of a wide variety of materials with excellent sensitivity. Instrument preparation was thus: radiofrequency power (RF) 1150W, nebulizer gas flow 0.70 L/min, argon gas pressure 60 psi, flush pump rate 25 rpm, analysis pump rate 50 rpm, auxiliary gas flow 0.5 L/min, coolant gas flow 12 L/min, purge gas flow normal and number of replicates 3 (Fig. 1).



Fig. 1: Biological samples preparation for determination of trace elements using inductively coupled plasma emission spectrometer (ICP/ES).

### Preparation of samples

The samples were prepared by accurately weighing 200–2000 mg of samples into a dry and clean Teflon digestion beaker; 6 mL of nitric acid ( $\text{HNO}_3$ ), 2 mL sulphuric acid ( $\text{H}_2\text{SO}_4$ ) and 2 mL perchloric acid ( $\text{HClO}_4$ ) were added to the beaker. Samples were digested on the hot plate at 120–150 °C for approximately 40 minutes. The resulting digest was not clear, so it was filtered through Whatman filtered paper no. 42. The filtered digest was transferred to a 50 mL plastic volumetric flask and made up to mark using deionized water. A blank digest was carried out in the same way.

### Reagents

Nitric acid (69% v/v) of super purity grade was from Romil, England, sulphuric acid (98% v/v) and perchloric acid (70% v/v) were supra-pure from Merck Germany. High purity water obtained from Millipore Milli-Q water purification system was used throughout the work.

### Calibration

The ICP-OES calibration was carried out with blank solution and three working standard solutions (20, 40, 60 and 80  $\mu\text{g/L}$ ) for 10 nm and 50 nm GNPs. Starting from a 1000 mg/L single standard solution, it was then diluted suitably using 1% nitric acid, aspirated and then nebulized using a quartz Meinhard micro-concentric type nebulizer into the argon plasma *via* a peristaltic pump with a flow rate of approximately 0.9–1.0 mL/min.

The mass spectral acquisitions were carried out using pulse-counting scanning mode with the following instrumental parameters: mass range scanned 190–220 m/z with 19 channels per mass, three points per peak and 10.24 ms dwell time on each isotopic mass. The instrument control, methods procedures and the data system, including calculations and statistics, were operated *via* a personal computer with Plasma Vision Software. Nitric acid (1%) blanks were run in between samples to correct the background levels.

### Histological investigation

Fresh portions of liver, heart, kidney and lung from each rat were cut rapidly, fixed in neutral buffered formalin (10%) and were then dehydrated with grades of ethanol (70, 80, 90, 95 and 100%). Dehydration was then followed by clearing the samples in two changes of xylene. Samples were then impregnated with two changes of molten paraffin wax, then embedded and blocked out. Paraffin sections (4–5  $\mu\text{m}$ ) were stained with haematoxylin and eosin (the conventional histological stain) according to Pearse (14). Stained sections of control and treated rats were examined for alterations in the hepatocytes for the presence of inflammatory, fatty change and Kupffer cells hyperplasia and necrosis.

## RESULTS

### Size and morphology of different GNPs

The 10 and 20 nm GNPs showed spherical morphology with a narrow particle size distribution when dispersed in the solution. The mean size for these GNPs was calculated from the TEM images. The mean measured size was  $9.45 \pm 1.33$  nm for 10 nm GNPs and  $20.18 \pm 1.80$  nm for 20 nm GNPs. Gold nanoparticles of 50 nm diameters, in contrast, were not spherical but hexagonal in TEM images (Figs. 2 and 3).

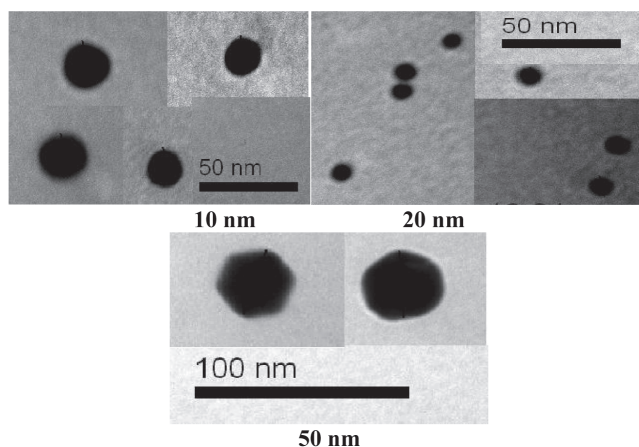


Fig. 2: Transmission electron microscopy images for different gold nanoparticle samples (15).

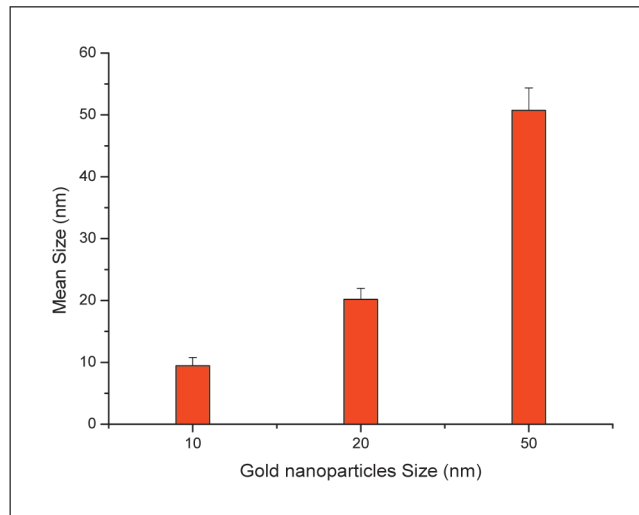


Fig. 3: The size of 10, 20 and 50 nm gold nanoparticles measured using transmission electron microscopy images (15–17).

We determined an accurate distribution of the GNP levels in the rats' blood using ICP-OES and the amounts of gold detected in blood were different. After the intraperitoneal administration of 10 and 50 nm GNPs at the dose of 50  $\mu\text{l}$  for three days, we found that the percentage normalization in-

creased in the blood with 50 nm GNPs compared with 10 nm GNPs (Fig. 4). This suggested that the administered 10 nm GNPs were absorbed into the systemic circulation and distributed into organs while the 50 nm GNPs were retained in the blood.

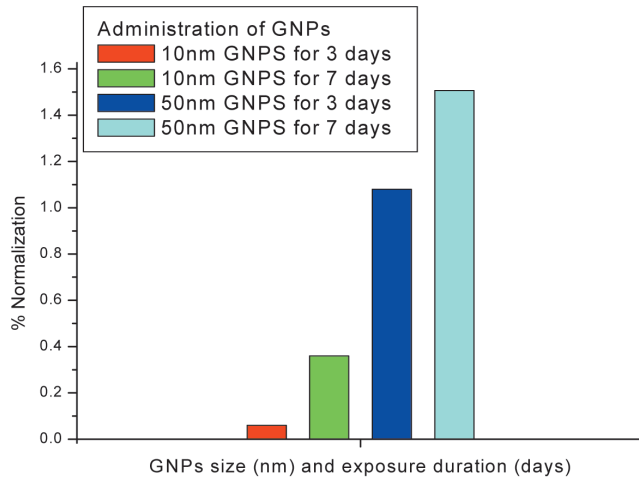


Fig. 4: The concentration of gold nanoparticles (GNPs) for 10 and 50 nm for three and seven days in the blood.

Figure 4 indicates the concentration of 10 and 50 nm GNPs for three days in the blood of rats. It became evident that the percentage normalization increased in the blood with 50 nm GNPs with the increase in exposure duration when compared with 10 nm GNPs.

The administration of smaller 10 nm GNPs induced prominent inflammation, central vein intima disruption, fatty change, Kupffer cells hyperplasia, cloudy swelling, cytoplasmic hyaline vacuolation, polymorphism, binucleation, karyopyknosis, karyolysis and necrosis (16, 17, 18) [Fig. 5].

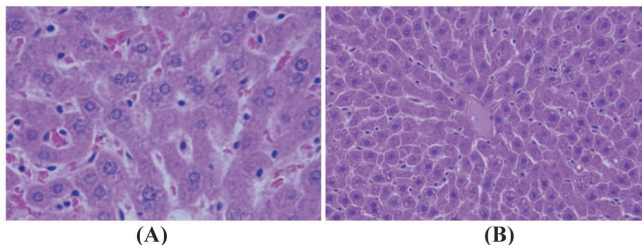


Fig. 5: A) Gold nanoparticle (GNP)-normal rat demonstrated normal hepatocytes. B) GNP-treated rat who received 50  $\mu$ l of 10 nm particles for seven days demonstrated Kupffer cells hyperplasia (16, 17, 18).

The administration of smaller 10 nm GNPs also induced disarray of heart muscle, haemorrhagic changes, chronic inflammatory cells infiltrated by small lymphocytes, cytoplasmic vacuolization and congested and dilated blood vessels, in addition to cardiac organ damage (19) [Fig. 6].

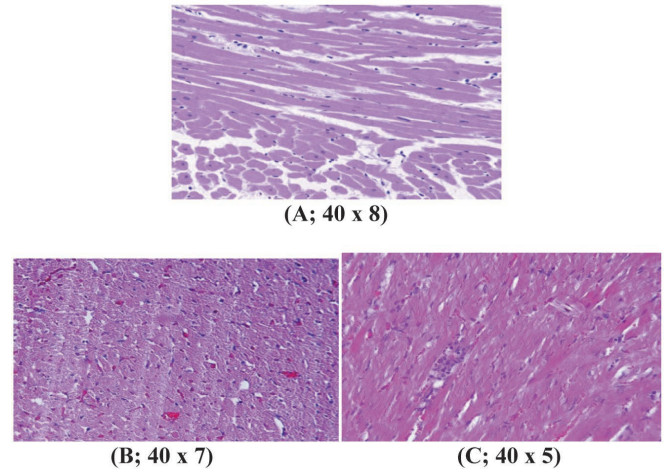


Fig. 6: A) Gold nanoparticle (GNP)-normal rats demonstrated benign, blunt-looking heart muscle with various heart muscle orientations and no pathological findings. B) GNP-treated rats who received 50  $\mu$ l of 10 nm particles for three days demonstrated extravasation of red blood cells with few scattered lymphocytic infiltrate. C) GNP-treated rats who received 50  $\mu$ l of 10 nm particles for seven days demonstrated scattered *foci* of haemorrhage with extravasation of red blood cells and a few scattered cytoplasmic vacuolization (19).

In the lung, the administration of smaller 10 nm GNPs induced pneumonia, fibrosis, chronic inflammatory cell infiltrates, congested and dilated blood vessels and haemosiderin granule and emphysema *foci* (20, 21) [Fig. 7].

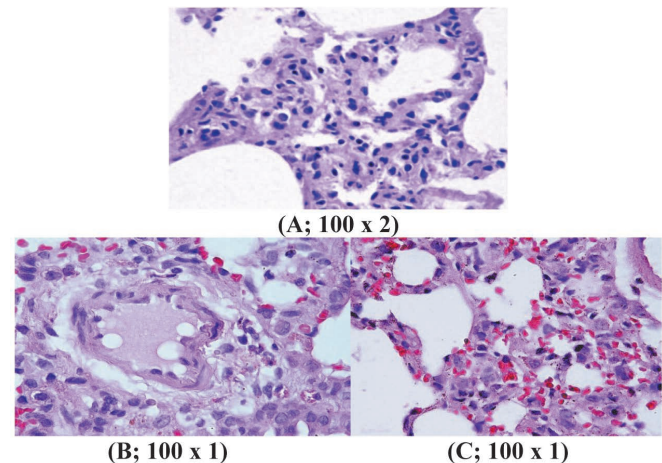


Fig. 7: A) Control group: Microscopic pictures show gold nanoparticle (GNP)-normal rats demonstrated well-formed and open alveoli with normal spate, few scattered small lymphocytes and minimal eosinophils. B) GNP-treated rats who received 50  $\mu$ l of 10 nm GNPs for three days demonstrated more diffuse interstitial pneumonia, dense inflammatory cell infiltrates of small lymphocytes, fibrosis and more prominent extravasation of red blood cells. C) GNP-treated rats who received 50  $\mu$ l of 10 nm particles for seven days demonstrated prominent chronic inflammatory cell infiltrates surrounded by dilated and congested blood vessels, scattered dense extravasation of red blood cells and *foci* of haemosiderin granules (20, 21).

The administration of smaller 10 nm GNPs induced renal cell cytoplasmic degeneration and nuclear destruction (22) [Fig. 8]. Vacuolization of the renal cells was seen and increased in severity in the renal tubules of rats who received 100  $\mu$ l of 10 or 20 nm GNPs, with less or no vacuolar degeneration with 50 nm particles. More vacuolar degeneration was observed in the renal cells of rats exposed to seven days than the ones exposed to three days (Fig. 8).

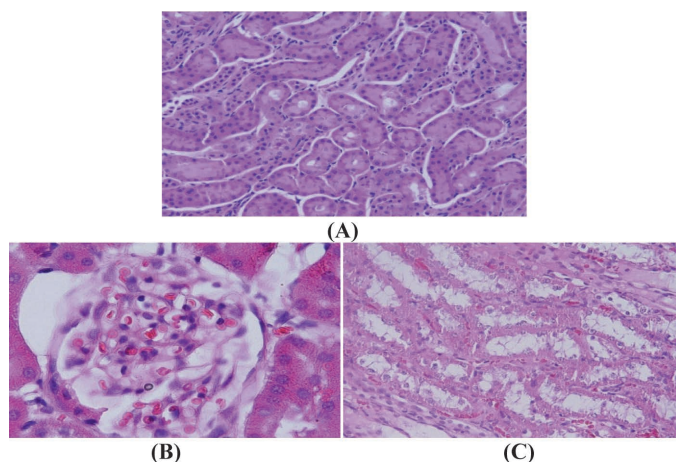


Fig. 8: A) Gold nanoparticle (GNP)-treated rat who received 100  $\mu$ l of 50 nm particles for seven days demonstrated normal renal tubules. B) GNP-treated rat who received 50  $\mu$ l of 10 nm particles for three days demonstrated glomerular congestion. C) GNP-treated rat who received 50  $\mu$ l of 10 nm particles for three days showed vacuolar degeneration (22).

## DISCUSSION

The high electron density and homogeneous shape and size of the GNPs make them highly conspicuous under the TEM (15–17). Cho *et al* have demonstrated that the gold concentration in organs is time-dependent after injection, and after intravenous injection of 13 nm GNPs, the gold was found in various organs just three days after injection. However, the blood gold levels were not increased proportional to the dose, indicating that GNPs are taken up and accumulate in organs (23).

Our method is identical or similar to what occurs in haemodialysis in kidney failure patients. Abdelhalim (16, 17, 20, 21) has indicated that the amount of accumulated GNPs in the organ reflected the toxicity. These histological alterations were size dependent, with smaller ones inducing the most effects and related to time of exposure of GNPs.

The liver and spleen are considered two dominant organs for bio-distribution and metabolism of GNPs (19, 24). If GNPs are larger than renal filtration cutoff, they are not excreted in urine; instead, they are eliminated from the blood by the reticuloendothelial system and thus tend to accumulate in the spleen and liver (24).

The proximal renal tubules are more affected than the distal ones. This could be because the proximal convoluted tubules are the primary sites of reabsorption and active trans-

port leading to higher concentration of the nanoparticles, especially the smaller ones in the epithelial lining of these tubules. Vacuolated degeneration is a result of ion and fluid homeostasis that lead to an increase of intracellular water (16). The vacuolated swelling of the cytoplasm of the renal cells of the GNP-treated rats might indicate acute and subacute renal injury induced by these nanoparticles (NPs). The organ distributions of GNPs are size dependent, and small GNPs of 5–15 nm have a wider organ distribution than that of large GNPs of 50–100 nm (13, 24). It has been found that GNPs with a long blood circulation time can accumulate in the liver and spleen and significantly affect the gene expression (25). Thus, the hepatotoxicity of GNPs may be attributed to accumulation of GNPs in liver.

The cytotoxicity and apoptosis in human breast epithelial MCF-7 cells using GNPs up to 200  $\mu$ g/mL for 24 hours have been examined. Concentration-dependent cytotoxicity and significant apoptosis in MCF-7 cells *via* p53, bax/bcl-2 and caspase pathways have been observed (26).

The results of this study indicate that the decrease in GNP size produces an exponential increase in surface area relative to volume, which may make the GNPs more self-reactive (*ie* may promote aggregation) and more prone to interactions with surrounding molecules (biological components). Moreover, increased uptake of GNPs may lead to accumulation in certain tissues, where the particles may interfere with critical biological functions (3).

The present results suggest that the larger 50 nm GNPs may be highly cleared *via* urine and bile. Nanoparticles for therapeutic use need to have a long retention time in order to encounter and interact with the desired target. However, a long retention time can result in toxic effects *in vivo*. Thus, route and rate of nanomaterial clearance is an important issue (17). The absorbed nanoparticles in the systemic circulation can be excreted through various routes, such as the kidneys or bile. Renal clearance of solid nano-sized materials is known to be influenced by particle size and surface charge (17). The smaller 10 nm GNPs have shown a propensity to accumulate in several rat organs following injection. The rat organ distribution of GNPs was size and exposure duration dependent; the smaller GNPs showed the most widespread organ accumulation and distribution, while the bigger 50 nm GNPs were retained in the blood for a long time.

This study gives a new therapeutic tool for blood cancer (leukaemia) by exposing blood to 50 nm GNPs and to a source of light. This idea is similar to the idea of haemodialysis, which is utilized in kidney failure patients. We can expose the blood of the patients with leukaemia *in vivo* after administration of 50 nm GNPs to any source of light and then the blood can be returned to the patient again to kill the malignant cells.

## CONCLUSIONS

The GNP levels were evaluated in several rat organs by ICP-OES. The GNPs levels increased in all the examined organs with G1A and G1B, while the GNP levels increased in rat

blood with G2A and G2B. Our results indicate that the smaller 10 nm GNPs are mostly taken up and accumulate in the different rat organs, suggesting the induced toxic effects, supported by histological investigation, while the larger 50 nm GNPs are retained in the rats' blood. This study suggests that the therapy of blood cancer might be done by using the larger GNPs.

#### AUTHOR'S NOTE

AMAK has interpreted and written the final draft of this manuscript and analysed the data. The animal model used in this study was obtained from the Laboratory Animal Center College of Pharmacy, King Saud University, Saudi Arabia. AMAK conceived the study and its design and obtained research grants for this study. The author declares that he has no competing interests. The author has read and approved the final manuscript.

#### ACKNOWLEDGEMENTS

The author would like to extend his sincere appreciation to the Deanship of Scientific Research at King Saud University for its funding of this research through the Research Group Project No. RGP-285.

#### REFERENCES

- Caruthers SD, Wickline SA, Lanza GM. Nanotechnological applications in medicine. *Curr Opin Biotechnol* 2007; **18**: 26–30.
- Kamat PV. Photochemical and photocatalytic aspects of metal nanoparticles. *J Phys Chem B* 2002; **106**: 7729–44.
- Kuwahara Y, Akiyama T, Yamada S. Facile fabrication of photoelectrochemical assemblies consisting of gold nanoparticles and a tris(2,2'-bipyridine)ruthenium(II)-viologen linked thiol. *Langmuir* 2001; **17**: 5714–6.
- Mirkin CA, Letsinger RL, Mucic RC, Storhoff JJ. A DNA-based method for rationally assembling nanoparticles into macroscopic materials. *Nature* 1996; **380**: 607–9.
- Huber M, Wei TF, Muller UR, Lefebvre PA, Marla SS, Bao YP. Gold nanoparticle probe-based gene expression analysis with unamplified total human RNA. *Nucleic Acids Res* 2004; **32**: e137–45.
- Kogan MJ, Olmedo I, Hosta L, Guerrero AR, Cruz LJ, Albericio F. Peptides and metallic nanoparticles for biomedical applications. *Nanomedicine* 2007; **2**: 287–306.
- El-Sayed IH, Huang X, El-Sayed MA. Selective laser photo-thermal therapy of epithelial carcinoma using anti-EGFR antibody conjugated gold nanoparticles. *Cancer Lett* 2006; **239**: 129–35.
- Zharov VP, Mercer KE, Galitovskaya EN, Smeltzer MS. Photothermal nanotherapeutics and nanodiagnostics for selective killing of bacteria targeted with gold nanoparticles. *Biophys J* 2006; **90**: 619–27.
- Hirsch LR, Stafford RJ, Bankson JA, Sershen SR, Rivera B, Price RE et al. Nanoshell-mediated near-infrared thermal therapy of tumors under magnetic resonance guidance. *Proc Natl Acad Sci USA* 2003; **100**: 13549–54.
- Liu WT. Nanoparticles and their biological and environmental applications. *J Biosci Bioeng* 2006; **102**: 1–7.
- Baptista P, Pereira E, Eaton P, Doria G, Miranda A, Gomes I. Gold nanoparticles for the development of clinical diagnosis methods. *Anal Bioanal Chem* 2008; **391**: 943–50.
- Pissuwan D, Valenzuela SM, Cortie MB. Therapeutic possibilities of plasmonically heated gold nanoparticles. *Trends Biotechnol* 2006; **24**: 62–7.
- Semmler-Behnke M, Kreyling WG, Lipka J. Biodistribution of 1.4- and 18-nm gold particles in rats. *Small* 2008; **4**: 2108–11.
- Pearse AE. *Histochemistry. Theoretical and applied*. Analytical technology. 4<sup>th</sup> ed, vol. 2. Edinburgh: Churchill-Livingstone; 1985.
- Abdelhalim MAK, Mady MM. Liver uptake of gold nanoparticles after intraperitoneal administration in vivo: a fluorescence study. *Lipids Health Dis* 2011; **10**: 195.
- Abdelhalim MAK, Jarrar BM. Gold nanoparticles administration induced prominent inflammatory, central vein intima disruption, fatty change and Kupffer cells hyperplasia. *Lipids Health Dis* 2011; **10**: 133.
- Abdelhalim MAK, Jarrar BM. Gold nanoparticles induced cloudy swelling to hydropic degeneration, cytoplasmic hyaline vacuolation, polymorphism, binucleation, karyopyknosis, karyolysis, karyorrhexis and necrosis in the liver. *Lipids Health Dis* 2011; **10**: 166.
- Abdelhalim MAK, Jarrar BM. Histological alterations in the liver of rats induced by different gold nanoparticle sizes, doses and exposure duration. *J Nanobiotechnology* 2012; **10**: 5.
- Abdelhalim MAK. The period effects of intraperitoneal administration of different gold nanoparticle sizes on heart tissue of rats using fluorescence measurements: in vivo. *Int J Phys Sci* 2011; **6**: 6166–70.
- Abdelhalim MAK. Exposure to gold nanoparticles produces pneumonia, fibrosis, chronic inflammatory cell infiltrates, congested and dilated blood vessels, and hemosiderin granule and emphysema foci. *J Cancer Sci Ther* 2012; **4**: 46–50.
- Abdelhalim MAK. Lung tissue alterations were size-dependent with smaller ones induced more effects and related with time exposure of gold nanoparticles. *J Cancer Sci Ther* 2012; **4**: 170–3.
- Abdelhalim MAK, Jarrar BM. Renal tissue alterations were size-dependent with smaller ones induced more effects and related with time exposure of gold nanoparticles. *Lipids Health Dis* 2011; **10**: 163.
- Cho WS, Cho M, Jeong J, Choi M, Cho HY, Han BS et al. Acute toxicity and pharmacokinetics of 13 nm-sized PEG-coated gold nanoparticles. *Toxicol Appl Pharmacol* 2009; **236**: 16–24.
- De Jong WH, Hagens WI, Krystek P, Burger MC, Sips AJ, Geertsma RE. Particle size-dependent organ distribution of gold nanoparticles after intravenous administration. *Biomaterials* 2008; **29**: 1912–9.
- Balasubramanian SK, Jittiwat J, Manikandan J, Ong CN, Yu LE, Ong WY. Bio distribution of GNPs and gene expression changes in the liver and spleen after intravenous administration in rats. *Biomaterials* 2010; **31**: 2034–42.
- Manar ES, Hendi AA. Gold nanoparticles induce apoptosis in MCF-7 human breast cancer cells. *Asian Pacific J Cancer Prev* 2012; **13**: 1617–20.